nature genetics

The mitochondrial DNA genetic bottleneck results from replication of a subpopulation of genomes

Timothy Wai, Daniella Teoli & Eric A Shoubridge

In mammals, mitochondrial DNA (mtDNA) sequence variants are observed to segregate rapidly between generations despite the high mtDNA copy number in the oocyte. This has led to the concept of a genetic bottleneck for the transmission of mtDNA[1–3], but the mechanism remains contentious. Several studies have suggested that the bottleneck occurs during embryonic development, as a result of a marked reduction in germline mtDNA copy number[4,5]. Mitotic segregation of mtDNAs during preimplantation[5], or during the expansion of primordial germ cells (PGCs) before they colonize the gonad[4,5], is thought to account for the increase in genotypic variance observed among mature oocytes from heteroplasmic mothers. This view has, however, been challenged by studies suggesting that the bottleneck occurs without a reduction in germline mtDNA content[6]. To resolve this controversy, we measured mtDNA heteroplasmy and copy number in single germ cells isolated from heteroplasmic mice. By directly tracking the evolution of mtDNA genotypic variance during oogenesis, we show that the genetic bottleneck occurs during postnatal folliculogenesis and not during embryonic oogenesis.

Hauswirth and Laipis proposed two hypotheses to explain the rapid segregation of neutral mtDNA variants between generations, first observed in Holstein cows: amplification of a small pool of mtDNAs at some point during oogenesis[1] or unequal partitioning of mtDNA in the early embryo[3]. We previously constructed a heteroplasmic mouse model carrying functionally neutral BALB and NZB mtDNA sequence variants to test these hypotheses[4]. As the genotypic variance measured in the PGCs of these mice was markedly less than the genotypic variance in postnatal germ cells or live offspring, we concluded that random genetic drift due to mitotic segregation of mtDNAs was likely sufficient to account for the increase in genotypic variance in mature oocytes. This hypothesis was apparently corroborated by morphological observations showing large differences (10^3–10^4) in mitochondrial number between PGCs and oocytes in humans[7].

Using quantitative PCR, Cao *et al.*[6] estimated mtDNA copy number in embryonic germ cells (identified by tissue nonspecific alkaline phosphatase (TNAP) activity) in embryonic day E7.5–E13.5 mouse embryos and failed to find any significant changes in mtDNA levels during embryonic germline development. They estimated mean mtDNA copy numbers of 1,500–3,000 and 100 mitochondria per cell. Thus, each mitochondrion was suggested to contain 15–30 mtDNAs, far more than had previously been reported in mammalian oocytes[8] or any mammalian cell. Without a change in germline mtDNA levels it would be virtually impossible for rapid segregation of mtDNA to occur during the expansion of the PGC population, and so they were forced to conclude that the genetic bottleneck was due to a subgroup of mtDNAs undergoing preferential replication during oogenesis. In sharp contrast, using a *Dppa3 (Stella)*-GFP mouse to isolate individual PGCs, Cree *et al.*[5] estimated ~200 copies of mtDNA in PGCs at E7.5 and ~1,300 copies at E14.5. Using a mathematical simulation they predicted that 70% of the mtDNA genotypic variance in the offspring of heteroplasmic mothers was generated by unequal portioning of mtDNA in the pre- and early postimplantation embryo, the remainder being generated during the mitotic expansion of the PGCs.

We reasoned that a definitive test of the role of germline mtDNA copy number in the genetic bottleneck would require direct measurements of both genotypic variance and mtDNA copy number during the development of the female germline, and a method to test for statistically significant changes in genotypic variance at each stage of oogenesis. We first isolated embryonic germ cells from heteroplasmic mice expressing enhanced green fluorescent protein (EGFP) from a modified *Pou5f1* (*Oct4*) promoter[9] and made single-cell measurements of mtDNA copy number and heteroplasmy. The reporter transgene eliminates the need for histochemical stains, which had previously been used to isolate the cells of the germline[10], but which confound mtDNA measurements made by quantitative PCR[5,6] (E.A.S. and T.W., unpublished data). In manually isolated EGPF-positive germ cells, we detected significant changes in mitochondrial DNA copy number during early oogenesis between E8.5 (mean ~280 copies, median 145), the earliest day at which we could unambiguously isolate these cells in the mouse strain we used, and E10.5 (~mean 2,800 copies, median 2200) (**Fig. 1**, top panel), similar to measurements made in PGCs isolated from the *Dppa3*-GFP mouse model[5]. *Dppa3* is one of the earliest markers of PGC specification, which occurs between E6.25 and E6.5 in the mouse[11]. E6.5 embryos contain about 910 cells[12], so if mtDNA replication were completely

Montreal Neurological Institute and Department of Human Genetics, McGill University, Montreal H3A 2B4, Canada. Correspondence should be addressed to E.A.S. (eric@ericpc.mni.mcgill.ca).

Received 10 June; accepted 19 September; published online 23 November 2008; doi:10.1038/ng.258

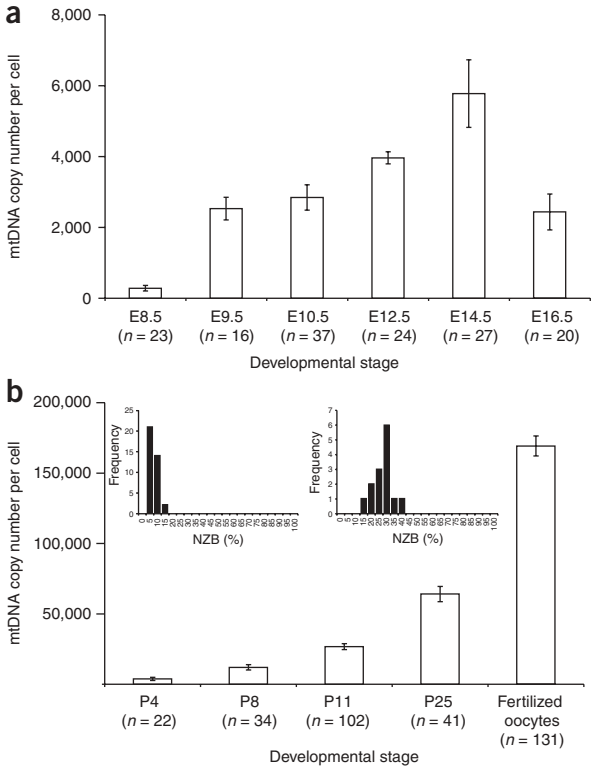

Figure 1 Changes in mtDNA copy number during female germline development. (**a**) Mean mitochondrial DNA copy number (± s.e.m.) measured in single embryonic germ cells isolated from OG2-BALB/NZB female embryos from E8.5 to E16.5. (**b**) Mean mitochondrial DNA copy number (± s.e.m.) measured in single postnatal oocytes isolated from live female offspring born to OG2-BALB/NZB mothers. Most of the oocytes from the P1–P4 animals are in primary follicles and most from the P29 animals are in secondary follicles. The insets show the frequency histograms of heteroplasmy levels in primary oocytes from a P1 mouse (left) and a P29 mouse (right), demonstrating the change in genotypic variance that is due to the mitochondrial genetic bottleneck.

arrested until this stage of development, individual cells would be expected to contain ~100 copies of mtDNA, assuming that about half of the mtDNAs in the zygote contribute to the embryo proper. Thus, it is likely that the resumption of mtDNA replication in early development occurs before PGC differentiation. By E14.5, when the PGCs have colonized the gonad, there are about 6,000 copies of mtDNA per cell. We observed significantly less mtDNA copy number variability in early PGCs than reported by Cree *et al.*[5] (s.d. 377 versus 699), a fact that we attribute to the manner in which we collected the cells. Manual isolation assures the exclusion of debris and doublets, which occurred at an unacceptable frequency in our experiments, even under the most stringent FACS gating parameters (data not shown). We conclude that there is in fact a severe decrease in mtDNA copy number in PGCs, at least 700-fold relative to the mtDNA copy number in fertilized oocytes, and that it increases 10- to 20-fold during the expansion of the PGC population before colonization of the gonad.

Notably, the large increase in mtDNA copy number during embryonic germline development does not lead to a concomitant increase in genotypic variance at any point during embryonic oogenesis when tested by a nonparametric test of equal variance (Methods and **Supplementary Fig. 1** online). It is important to note that our analyses of genotypic variance make no a priori assumptions regarding the organization of the mitochondrial nucleoid, the nature or number of segregating units, or the number of germline mitotic divisions required for the genesis of mature oocytes. Rather, these analyses simply allow us to detect increases in genotypic variance, which is a direct measure of the segregation of mtDNA sequence variants. In this regard, our results directly contradict those of Cree *et al.*[5], who did not examine levels of heteroplasmy directly in germ cells, but rather based their prediction of the evolution of heteroplasmy variance in early embryological development on a mathematical simulation. Actual measurements of genotypic variance in early PGCs in this study and in our previous study[4] are inconsistent with significant mtDNA segregation before implantation, and even when we did all possible pairwise comparisons at different stages of embryonic oogenesis, we failed to find significant differences in genotypic variance (**Supplementary Fig. 1**). We conclude that despite the severe reduction in mtDNA copy number, the mitochondrial genetic bottleneck does not occur during embryonic oogenesis.

We extended our analyses postnatally and discovered an inequality of genotypic variance (**Supplementary Table 1** online) between all groups of germ cells containing more than 10,000 copies of mtDNA per cell (mature ovulated oocytes, primary oocytes in secondary follicles) and those groups of germ cells containing less than 10,000 copies of mtDNA per cell (PGCs, oogonia, primary oocytes in primordial follicles) (**Fig. 1** and **Supplementary Fig. 1**). These results indicate that the genetic bottleneck must be the result of the selective replication of a random subset of mtDNA templates during the growth and maturation of the ovarian follicles. This likely starts in the primordial follicles, as this subpopulation of mtDNAs would have to expand significantly in order for us to detect a change in genotypic variance in the oocytes derived from secondary follicles.

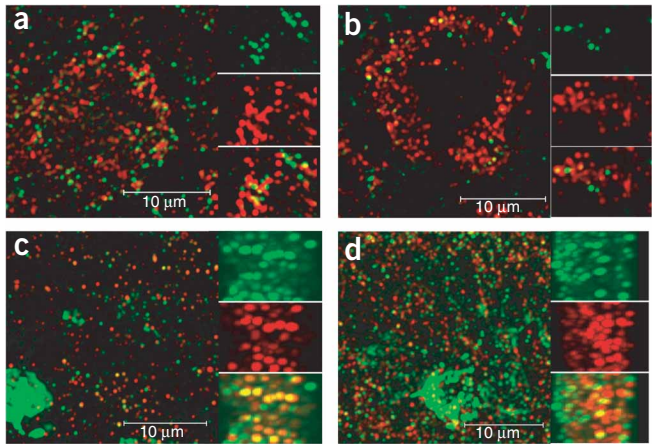

Figure 2 Replicating mtDNA visualized *in vivo* by incorporation of BrdU. (**a**,**b**) BrdU incorporation studies in primary oocytes labeled for 24 h (**a**) or 2 h (**b**) show that replicating mtDNAs (green) represent a small subgroup of all Tfam-positive mtDNA nucleoids (red). (**c**,**d**) BrdU labeling in sections of neonatal heart (**c**) and in sections of neonatal liver (**d**) are shown for comparison. The degree to which BrdU punctae colocalize with Tfam punctae is tissue specific. Sections of primary oocytes show the least colocalization compared to neonatal heart or liver sections. Confocal micrographs are represented as merged maximum projections. Insets to the right in each panel show close-ups of individual channels and merged maximum projections. Videos showing three-dimensional views of the merged maximum projection close-ups for primary oocytes and neonatal heart are available as **Supplementary Videos 1** and **2** online (primary oocyte and neonatal heart, respectively).

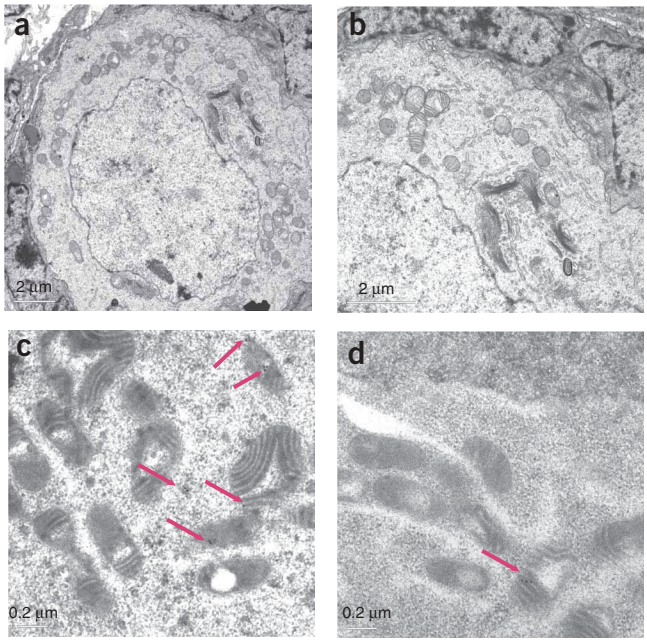

Figure 3 Transmission electronmicroscopy and immunogold labeling in primary oocytes. (**a**,**b**) Mitochondria are asymmetrically distributed about the Balbiani body (**a**, ×6,000) and are cristae poor (**b**, ×10,000). (**c**,**d**) No more than 2 foci of either BrdU (**c**) or Tfam (**d**) were observed in cross-sections of oocyte mitochondria after immunogold labeling (×43,000). Arrows point to gold particles.

To confirm these genetic observations, we injected early postnatal mice (postnatal day P1 to P4) with the thymidine analog BrdU to label replicating mtDNA. Following short (2 h) and long BrdU pulses (24 h), we harvested tissues for sectioning and immunohistochemical analyses. mtDNAs labeled with BrdU represent a small fraction of the total cellular nucleoid content in oocytes in both primordial and primary follicles as visualized with antibodies against either TFAM (**Fig. 2**), mt-SSB (**Supplementary Fig. 2** online) or POLG (**Supplementary Fig. 3** online), markers of the mammalian nucleoid[13], confirming the predictions of the genetic analysis. TFAM-positive punctae show a reduced degree of co-localization to BrdU-positive punctae in ovarian sections (**Fig. 2a**,**b**), as compared to other tissues such as the heart (**Fig. 2c**,**d**), and particularly when compared to cultured cells (**Supplementary Fig. 2**), an observation that was recapitulated using POLG and mt-SSB antibodies (**Supplementary Fig. 1**). Although it is not clear why established markers of the mitochondrial nucleoid such as TFAM variably colocalize with foci of BrdU incorporation, there could be a number of explanations. We have previously shown that TFAM binds DNA nonspecifically with nanomolar affinity and can completely coat and compact plasmid DNA molecules[14]. It is likely that this tight association needs to be modulated in order for the replication machinery to gain access to the DNA template, leading to reduced TFAM content on replicating mtDNAs, or to a change in epitope accessibility. It is worth noting that although BrdU-positive, TFAM-negative foci have been previously observed by immunocytochemistry in transformed cultured cells[15], this observation has generally been ignored. It is entirely possible that this population represents actively replicating templates, which subsequently acquire additional TFAM and become compacted when replication terminates. Thus the relative proportion of nucleoids that stain positive for both TFAM and BrdU might simply reflect the rate of mtDNA replication in a particular cell or tissue.

Immuno-electron microscopy in the same postnatal ovaries showed that both anti-TFAM and anti-BrdU immunoreactivity were confined to the mitochondrial compartment (**Fig. 3c**,**d**). Using either antibody, we rarely observed more than a single focus of immunoreactivity (which we interpret as a nucleoid) in an individual mitochondrion (range 0–2), consistent with the idea that mitochondria in oocytes contain a small number of mtDNAs.

Coincident with the mitochondrial genetic bottleneck is the appearance of the Balbiani body, which contains Golgi elements surrounded by mitochondria and endoplasmic reticulum[16,17]. This structure is evolutionarily conserved and has been suggested to have a role in mitochondrial inheritance[18], so we asked whether the Balbiani body might influence the selection templates for replication. We observed a heterogeneous distribution of TFAM-positive mtDNA nucleoids located primarily about the GM130-positive Bb in primary oocytes (**Figs. 3a**,**b** and **4a**). Following maturation through to the secondary follicle stage, the distribution of mitochondria and mtDNA nucleoids became more homogeneous and the Balbiani body dispersed (**Fig. 4b**). However, immunohistochemical analyses at the electron- or confocal-microscope level (data not shown and **Supplementary Fig. 4** online) showed that replicating mtDNAs did not exclusively colocalize with the Balbiani body. Thus, the Balbiani body does not have an obvious role in the segregation of mammalian mitochondrial DNA. It is, however, possible that mitochondria are moving in and out of the Balbiani body, so we cannot entirely exclude a role for this structure in the selection of mtDNA templates for replication.

If the genetic bottleneck does not occur during embryonic oogenesis, what purpose is served by the severe reduction in mtDNA copy number that occurs in the earliest PGCs? Recent studies[19,20] have suggested that mtDNA undergoes purifying selection in the germline, eliminating severe mutations. Successive backcrosses of a mutant line carrying a severe frameshift mutation in ND6 led to the rapid elimination of the mutant genome within three generations[19], demonstrating that this filter can extinguish deleterious mutations well below the mutant loads that would be predicted to cause a biochemical deficit at the cellular level. If the mitochondrial genetic bottleneck were responsible for this selective elimination, one would predict that the genotypic variance observed in mature oocytes carrying such mutations would be reduced. To test this, we compared the genotypic variance reported in 12 oocytes from the mouse segregating a deleterious ND6 frameshift mutation[19] with that which we had

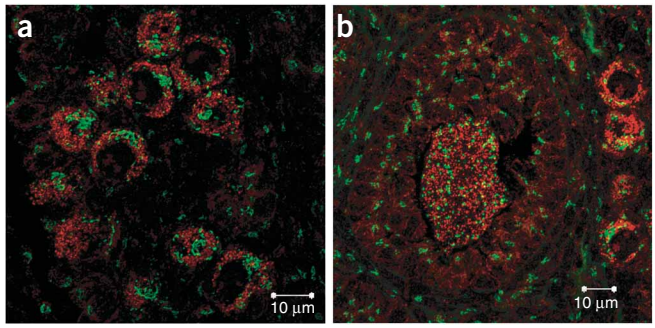

Figure 4 The distribution of mtDNA nucleoids in primary oocytes. (**a**) Tfam-positive mtDNA nucleoids (red) are asymmetrically distributed about the GM130-positive Balbiani body (green) in primary oocytes. (**b**) By the secondary follicle stage, oocytes regain their homogeneous distribution following the dispersion of the Balbiani body. Confocal micrographs are presented as merged maximum projections.

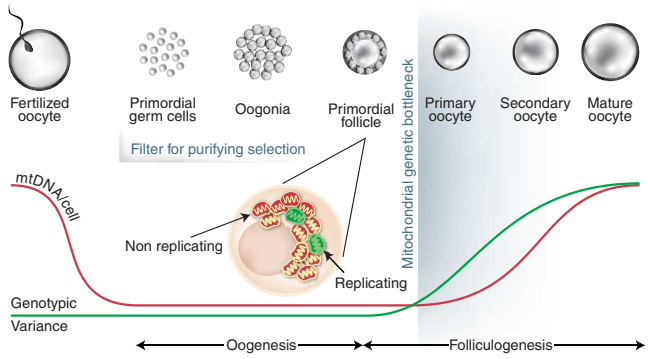

Figure 5 Model for the transmission of mtDNA in the female germline. The postnatal mitochondrial genetic bottleneck during folliculogenesis rapidly segregates sequence variants that pass through the filter for purifying selection at the physical bottleneck for mtDNA in primordial germ cells.

previously measured in ovulated oocytes, embryos or live offspring from our heteroplasmic mice (data not shown), and found no statistically significant differences. As purifying selection decreases genetic variance, this comparison suggests that the mechanism responsible for the selective elimination of severe mutations acts before the genetic bottleneck determined in our mouse model.

The results we present here allow us to propose a model for the transmission of mtDNA (**Fig. 5**). The high mtDNA copy number in mature oocytes (~175,000 copies, likely organized at 1 to 2 copies per organelle) can be viewed as a genetic device to ensure distribution of mitochondria to the cells of the early embryo at a time when mitochondrial biogenesis is arrested. Resumption of mitochondrial biogenesis by E6.5 results in a 10- to 20-fold increase in mtDNA copy number from the emergence of primordial germ cells until colonization of the gonad at E13.5. Although there is no measurable segregation of neutral sequence variants at this time, a physical bottleneck (~200 mtDNAs) in the earliest PGCs enables selection against severely deleterious mtDNA mutations at the level of the organelle, possibly through replicative competition[21]. The genetic bottleneck for neutral (and less deleterious mtDNA sequence variants that are associated with most human disease) occurs during folliculogenesis, in early postnatal life, as a result of replication of a subpopulation of mtDNAs. In this way, mutations that escape the filter for purifying selection are rapidly segregated and exposed to selection at the level of the organism in individual maternal lineages. It remains to be determined how a subpopulation of mtDNAs is preferentially replicated in early postnatal oocytes, but the mechanism could involve turning off replication in the majority of organelles.

METHODS

Transgenic mice. We obtained mice carrying the *GOF18deltaPE* transgene, which is a specific marker of PGCs after E8.5, from H. Scholer[9]. The males (C57BL/6 background) were crossed to Balb/c heteroplasmic females[4]. The F3 *GOF18deltaPE*$^{+/+}$ males were backcrossed to F2 *GOF18deltaPE*$^{+/+}$ heteroplasmic transgenic females, generating the OG2-BALB/NZB line. Genotyping for the presence of the transgene[9] and sex genotyping[22] were done as previously described. The animal studies were approved by the McGill University Animal Care Committee.

Isolation of cleavage stage embryos, oocytes and single embryonic germ cells. Early embryos (E0.5 to E3.0) were flushed from oviducts following natural timed matings of OG2-BALB/NZB mice. Postnatal oocytes were harvested from individual follicles using tungsten needles. We isolated Female PGCs from OG2-BALB/NZB E8.5 to E14.5 embryos by disaggregating the embryo under an epifluorescencent dissecting microscope and manually pipetting individual germ cells expressing GFP. Disaggregation was done by enzymatic digestion with collagenase type 1A (Sigma) and trypsin-EDTA (0.25%) in a 1:1 ratio (total volume 50 µl) at 37 °C for 5 min, inverting the microfuge tube every 30 s. Single cell separation was achieved by pipetting up and down and by vortexing briefly. We arrested enzymatic digestion by adding a tenfold excess of cold PBS + 0.01% BSA. Individual cells or embryos were washed three times in Ca^{2+}- and Mg^{2+}-free PBS and finally transferred into a PCR tube containing 10 µl of the washing solution. We lysed the cells by three rounds of freeze-thawing (heating at 99 °C with immediate freezing in liquid nitrogen) as previously described[23]. Freeze-thawing in PCR buffer or buffers containing detergents had a deleterious effect on the amplification efficiency of the MT9/11 quantitative real-time PCR assay.

Mitochondrial DNA quantitation by quantitative real-time PCR (Q-PCR). We used single-cell lysates as the template and carried out Q-PCR in triplicate using MT9 Forward and MT11 Reverse primers (**Supplementary Table 2** online). Absolute mtDNA copy number in a 1 µl aliquot of single cell lysates was calculated using a standard curve derived from Q-PCR amplifications of 10 to 10^6 copies of a region of mtDNA subcloned into PCR2.1-TopoTA vector using primers MT12 and MT13 (**Supplementary Table 2**).

The plasmid standard was constructed by cloning a region of mtDNA amplified using primers MT12 (forward) and MT13 (reverse) followed by cloning into PCR2.1-TopoTA (Invitrogen). We determined the MT12/13 plasmid standard concentration by UV spectroscopy and agarose gel with a high-mass ladder. Q-PCR reactions using MT9 (forward) and MT11 (reverse) primers were run using DNA Faststar Master Plus Sybr Green (Roche) on the Rotorgene 3000 (Corbett) according to the following conditions: 35 cycles, denaturation at 95 °C for 10 s, annealing at 60 °C for 15 s, and extension at 72 °C for 20 s. Melt-curve analyses reported on the specificity of the PCR products that were amplified. Post-run analyses of amplification efficiency were performed and corrected using Rotorgene software and LINREGPCR[24] programs. We tested all samples and standards in triplicate using 1 µl of template per 10 µl PCR reaction. This Q-PCR system could detect as few as ten copies of a standard DNA template and the linear regression analysis of all standard cuves for sample with copy number between 10 and 10^9 showed a high correlation coefficient (r^2 = 0.999). The Q-PCR assay was validated by slot-blotting serially diluted MT12/13 plasmid standards as well as pooled ovulated oocytes from OG2-BALB/NZB females (data not shown). Rho zero cells were as negative controls.

Mitochondrial DNA genotyping. We determined the proportion of NZB mtDNA in single cells essentially as previously described[25], except that we first carried out nonradioactive nested PCR reactions using primers MT12 (forward) and MT13 (reverse) for 20 cycles in single-cell lysates obtained from embryonic and neonatal germ cells. We subsequently amplified 2 µl of these PCR products amplified using MT9 and MT10 (5′CTGCTTCAGTT GATCGTGGGT3′) in a 'last cycle hot' PCR reaction.

BrdU labeling. Neonatal females (P1 to P4) were subcutaneously injected with 100 mg BrdU per kilogram body weight (Roche) and killed after 2 or 24 h. Tissues were immediately harvested and prepared for immunohistochemistry.

Confocal microscopy and immunohistochemistry. For immunocytochemistry, C2C12 mouse cells were grown in DMEM (Hyclone) containing 10% FBS and plated on coverslips before fixation in 4% paraformaldehyde. For immunohistochemistry, we froze tissues harvested from BrdU-injected pups in OCT freezing medium. Cryosections (10 µm) were incubated with various combinations of mouse anti-BrdU (Roche, 1/10), mouse anti-GM130 (BD Biosciences, 1/250), rabbit anti-TFAM (gift of B. Kaufman, 1/250), anti-mtSSB (gift of M. Zeviani, 1/250) and anti-POLG (gift of W. Copeland, 1/250) primary antibodies, followed by goat anti-mouse Alexa488 and goat anti-rabbit Alexa568 (Molecular Probes, 1/500). Parallel negative controls omitted the primary antibodies. In some instances a series of fluorescent confocal images (Z stacks) were acquired with a LSM 510 meta confocal microscope (Zeiss Oberkochen) and visualized using a 543-nm helium-neon laser and 488-nm argon laser lines, respectively. Slides were imaged in Z series every 0.20 µm and Z images were deconvolved according to empirically determined point spread functions with Huygens Professional 3.0 software.

Transmission electron microscopy and immunohistochemistry. Ovaries taken from neonatal mice injected with BrdU (see above) were fixed and processed in either Epon (Hexion Specialty Chemicals) or LR White acrylic resin (London Resin Company) as previously described[26]. For transmission electron microscopy, selected regions were trimmed, and ultra-thin sections (80 nm) were placed on Formvar-coated nickel grids. Post-embedding immunolabeling was done on the grid-mounted sections as described previously[26]. Grid-mounted tissue sections were processed for colloidal-gold immunocytochemistry by incubation of the sections with undiluted primary antibodies against either BrdU (Roche) or Tfam, after which immunolabeling patterns were visualized by incubation with protein A–colloidal gold complex (18 nm; Jackson ImmunoResearch Laboratories). Briefly, the grids were incubated for 10 min with 1% BSA in PBS, followed by incubation with primary antibody for 1 h, blocking with 1% BSA in PBS, and then incubation with protein A–gold for 30 min. The grids were then rinsed with distilled water, air-dried and stained conventionally for transmission electron microscopy using uranyl acetate and lead citrate. We recorded the images using a Philips FEI Tecnai 12 transmission electron microscope operating at 120 kV.

Statistical testing. The non-normal (beta) heteroplasmy distributions in germ cells, embryos or offspring violate the assumptions of the parametric F-test for equal variances. Hence we used the Levene test and bootstrapped Levene test for equal variances using the Brown and Forsythe correction[27]. Head-to-head comparisons of all known tests of equal variances have shown that the Levene test is the most robust and powerful, and the least likely to commit type 2 errors[28,29]. Nevertheless, we tested the power and robustness of both the bootstrapped and nonbootstrapped Brown-Forsythe corrected Levene tests, validating them both by the Monte Carlo permutation test on simulated data as well as on actual datasets wherein previously established differences in genotypic variance had been proven[30]. The results indicated that in the event of small sample sizes ($n > 5$), the bootstrapped version of the Levene test is more reliable. We carried out pairwise comparisons of the genotypic variance of groups of cells sampled at various points during germline development using both the bootstrapped and nonbootstrapped Levene tests; *P* values are reported in **Supplementary Table 1** (**Supplementary Fig. 1**).

Note: Supplementary information is available on the Nature Genetics website.

ACKNOWLEDGMENTS

We thank L. Villeneuve for help with confocal microscopy; J. Mui for assistance with electron microscopy; T. Johns, F. Jones and D. Sabour for technical assistance; and J. Correa for statistical design. We are grateful for antibodies directed against TFAM (B. Kaufman, MNI), mt-SSB (M. Zeviani, Instituto Carlo Besta) and POLG (W. Copeland, US National Institutes of Health). The OCT4Δ PE-EGFP mice were obtained from H.R. Scholer (University of Pennsylvania). This research was supported by the Canadian Institutes of Health Research and the US National Institutes of Health. E.A.S. is an International Scholar of the Howard Hughes Medical Institute.

AUTHOR CONTRIBUTIONS

T.W. and E.A.S. designed the study and wrote the manuscript. D.T. performed genotyping, and T.W. did all other experiments.

Published online at http://www.nature.com/naturegenetics/
Reprints and permissions information is available online at http://npg.nature.com/reprintsandpermissions/

1. Hauswirth, W.W. & Laipis, P.J. Mitochondrial DNA polymorphism in a maternal lineage of Holstein cows. *Proc. Natl. Acad. Sci. USA* **79**, 4686–4690 (1982).
2. Olivo, P.D., Van de Walle, M.J., Laipis, P.J. & Hauswirth, W.W. Nucleotide sequence evidence for rapid genotypic shifts in the bovine mitochondrial DNA D-loop. *Nature* **306**, 400–402 (1983).
3. Laipis, P.J., Van de Walle, M.J. & Hauswirth, W.W. Unequal partitioning of bovine mitochondrial genotypes among siblings. *Proc. Natl. Acad. Sci. USA* **85**, 8107–8110 (1988).
4. Jenuth, J.P., Peterson, A.C., Fu, K. & Shoubridge, E.A. Random genetic drift in the female germline explains the rapid segregation of mammalian mitochondrial DNA. *Nat. Genet.* **14**, 146–151 (1996).
5. Cree, L.M. *et al.* A reduction of mitochondrial DNA molecules during embryogenesis explains the rapid segregation of genotypes. *Nat. Genet.* **40**, 249–254 (2008).
6. Cao, L. *et al.* The mitochondrial bottleneck occurs without reduction of mtDNA content in female mouse germ cells. *Nat. Genet.* **39**, 386–390 (2007).
7. Jansen, R.P. Germline passage of mitochondria: quantitative considerations and possible embryological sequelae. *Hum. Reprod.* **15** Suppl 2, 112–128 (2000).
8. Michaels, G.S., Hauswirth, W.W. & Laipis, P.J. Mitochondrial DNA copy number in bovine oocytes and somatic cells. *Dev. Biol.* **94**, 246–251 (1982).
9. Yeom, Y.I. *et al.* Germline regulatory element of Oct-4 specific for the totipotent cycle of embryonal cells. *Development* **122**, 881–894 (1996).
10. Chiquoine, A.D. The identification, origin, and migration of the primordial germ cells in the mouse embryo. *Anat. Rec.* **118**, 135–146 (1954).
11. Hayashi, K., de Sousa Lopes, S.M. & Surani, M.A. Germ cell specification in mice. *Science* **316**, 394–396 (2007).
12. Snow, M.H. Gastrulation in the mouse: Growth and regionalization of the epiblast. *J. Embryol. Exp. Morphol.* **42**, 293–303 (1977).
13. Kucej, M. & Butow, R.A. Evolutionary tinkering with mitochondrial nucleoids. *Trends Cell Biol.* **17**, 586–592 (2007).
14. Kaufman, B.A. *et al.* The mitochondrial transcription factor TFAM coordinates the assembly of multiple DNA molecules into nucleoid-like structures. *Mol. Biol. Cell* **18**, 3225–3236 (2007).
15. Legros, F., Malka, F., Frachon, P., Lombes, A. & Rojo, M. Organization and dynamics of human mitochondrial DNA. *J. Cell Sci.* **117**, 2653–2662 (2004).
16. Kloc, M., Bilinski, S. & Etkin, L.D. The Balbiani body and germ cell determinants: 150 years later. *Curr. Top. Dev. Biol.* **59**, 1–36 (2004).
17. Pepling, M.E., Wilhelm, J.E., O'Hara, A.L., Gephardt, G.W. & Spradling, A.C. Mouse oocytes within germ cell cysts and primordial follicles contain a Balbiani body. *Proc. Natl. Acad. Sci. USA* **104**, 187–192 (2007).
18. Cox, R.T. & Spradling, A.C. A Balbiani body and the fusome mediate mitochondrial inheritance during *Drosophila* oogenesis. *Development* **130**, 1579–1590 (2003).
19. Fan, W. *et al.* A mouse model of mitochondrial disease reveals germline selection against severe mtDNA mutations. *Science* **319**, 958–962 (2008).
20. Stewart, J.B. *et al.* Strong purifying selection in transmission of mitochondrial DNA. *PLoS Biol.* **6**, e10 (2008).
21. Shoubridge, E.A. & Wai, T. Sidestepping mutational meltdown. *Science* **319**, 914–915 (2008).
22. Zhang, Y.H. *et al.* Mouth cell collection device for newborn mice. *Mol. Genet. Metab.* **89**, 164–167 (2006).
23. El Shourbagy, S.H., Spikings, E.C., Freitas, M. & St John, J.C. Mitochondria directly influence fertilisation outcome in the pig. *Reproduction* **131**, 233–245 (2006).
24. Ramakers, C., Ruijter, J.M., Deprez, R.H. & Moorman, A.F. Assumption-free analysis of quantitative real-time polymerase chain reaction (PCR) data. *Neurosci. Lett.* **339**, 62–66 (2003).
25. Battersby, B.J., Redpath, M.E. & Shoubridge, E.A. Mitochondrial DNA segregation in hematopoietic lineages does not depend on MHC presentation of mitochondrially encoded peptides. *Hum. Mol. Genet.* **14**, 2587–2594 (2005).
26. McKee, M.D. & Nanci, A. Postembedding colloidal-gold immunocytochemistry of noncollagenous extracellular matrix proteins in mineralized tissues. *Microsc. Res. Tech.* **31**, 44–62 (1995).
27. Brown, M.B. & Forsythe, A.B. Robust tests for the equality of variances. *J. Am. Stat. Assoc.* **69**, 364–367 (1974).
28. Pan, G. Confidence intervals for comparing two scale parameters based on Levene's statistics. *J. Nonparam. Stat.* **14**, 459–476 (2007).
29. Lim, T.-S. & Loh, W.-Y.Acomparison of tests of equality of variances. *Comput. Stat. Data Anal.* **22**, 287–301 (1995).
30. Battersby, B.J., Loredo-Osti, J.C. & Shoubridge, E.A. Nuclear genetic control of mitochondrial DNA segregation. *Nat. Genet.* **33**, 183–186 (2003).